Electron CHanneling ORientation Determination (eCHORD): An original approach to crystalline orientation mapping

C. Lafond, Thierry Douillard, Sophie Cazottes, Philippe Steyer, Cyril Langlois

electron CHanneling ORientation Determination (eCHORD): an original approach to crystalline orientation mapping

C.Lafond[1], T. Douillard[1], S. Cazottes[1], P. Steyer[1], C. Langlois[1*]

Université de Lyon, INSA-Lyon, MATEIS CNRS UMR5510, 7 avenue Jean Capelle, 69621 Villeurbanne (France)

* corresponding author

Keywords : Orientation mapping, SEM, Electron Channeling, EBSD

Highlights :

- A proof of concept for an orientation mapping in the SEM is proposed.
- This new approach is based on electron channeling.
- Excellent agreement compared with EBSD maps was obtained on an aluminium alloy sample.

Abstract

We present a proof-of-concept attesting the feasability to obtain orientation maps of polycrystalline materials within a conventional Scanning Electron Microscope (SEM) using a standard goniometer and Back Scattered Electron (BSE) detector. The described method is based on the analysis of the contrast variation of grains due to the channeling of incident electrons on a rotating sample. On each pixel of the map, experimental intensity profiles as a function of the rotation angle are obtained and compared with simulated ones to retrieve the orientation. From first results on aluminum polycrystals, the angular resolution is estimated to be better than one degree.

1. Introduction

In the past ten years, the EBSD and Transmission Kikuchi Diffraction (TKD) techniques have been modified to improve spatial and angular resolutions as well as the indexation speed. For instance, High Resolution-EBSD (HR-EBSD) [1] provides a high angular resolution at the expense of time and heavy data processing whereas TKD-on axis [2] procedure on Transmission Electron Microscopy (TEM) samples allows obtaining a better spatial resolution together with a high indexation speed. Orientation maps can also be obtained by a completely different approach using images presenting channeling contrast, as demonstrated in the article by Langlois *et al.* [3]. In this paper, an ion beam was used to produce secondary electron images, taking benefits from a strong channeling phenomenon with a high secondary electron yield. If well-defined orientation maps were obtained by **i**on **Ch**anneling **Or**ientation **D**etermination (iCHORD) on cubic materials, the ion beam may intrinsically affect the sample by milling, implantation or amorphisation. Such negative issues can be overcome with an electron beam. This paper demonstrates how the iCHORD method can be extended to electron channeling contrast to recover crystalline orientations in a standard SEM. This method is called **eCHORD** and opens new possibilities for fast and spatially resolved crystallographic mapping.

2. From ion to electron channeling modelling

The channeling contrast is directly related to the orientation of the crystal relative to the incident beam [4]. Following this principle, it has been shown that recording the intensity variation of a crystal in rotation around the z axis of the goniometer (tilted with respect to the

beam) may result in an unambiguous intensity profile for a given orientation [3]. The corresponding acquisition setup has been adapted for electrons as described in Fig.1. Serial imaging was performed using a Gemini I SEM column (Carl Zeiss Microscopy GmbH, Oberkochen, Germany) equipped with a retractable standard 4 Quadrant solid-state Detector (Namely 4Q-BSD). The electron accelerating voltage was set to 15kV and the sample tilt to 10°. The so-called High Current Mode was activated. With the use of an objective lens aperture of 60 microns, a beam current of 2nA was measured. A working distance of 6 mm was chosen to collect a maximum of BSE on the detector.

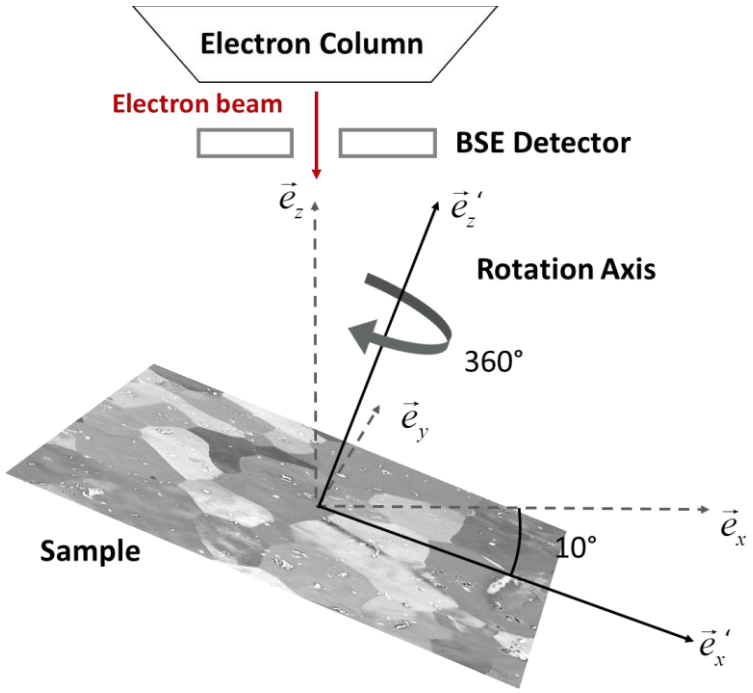

Figure1: Experimental eCHORD setup: the sample is 10° tilted and rotated from 0° to 360°. A BSE detector records the backscattered electron intensity at each rotation step.

For each rotation step of 1°, an image is collected from 0° to 360°. All 360 images are stacked together in FIJI software [5]. The stack is numerically treated using Xlib library

(developped by Beat Münch [6]) for denoising and edge detection as well as MultiStackReg (developped by Brad Busse [7]) for image alignment. Noise is removed from raw images using the Tschumperlé & Deriche anisotropic diffusion algorithm [8] implemented in Xlib with default parameters. This algorithm allows removing the noise while preserving the edges i.e. the grain boundaries. Concerning images alignment, the process is in three steps: i) edge detection using Canny algorithm [9], ii) alignment of the edge-detected stack with affine transformations [10], saving the set of alignment parameters, iii) original stack alignment by loading this parameters set. The alignment algorithm used here does not require any experimental information about rotation, tilt or stage drift; it will automatically find the best affine transformation to align all the images of the series to the initial one. In the final stack, a given pixel contrast changes throughout the stack due to the electron channeling. These intensity variations are plotted as a function of the rotation angle in order to obtain an intensity profile for each (X, Y) point of the image stack (see Fig.2.b).

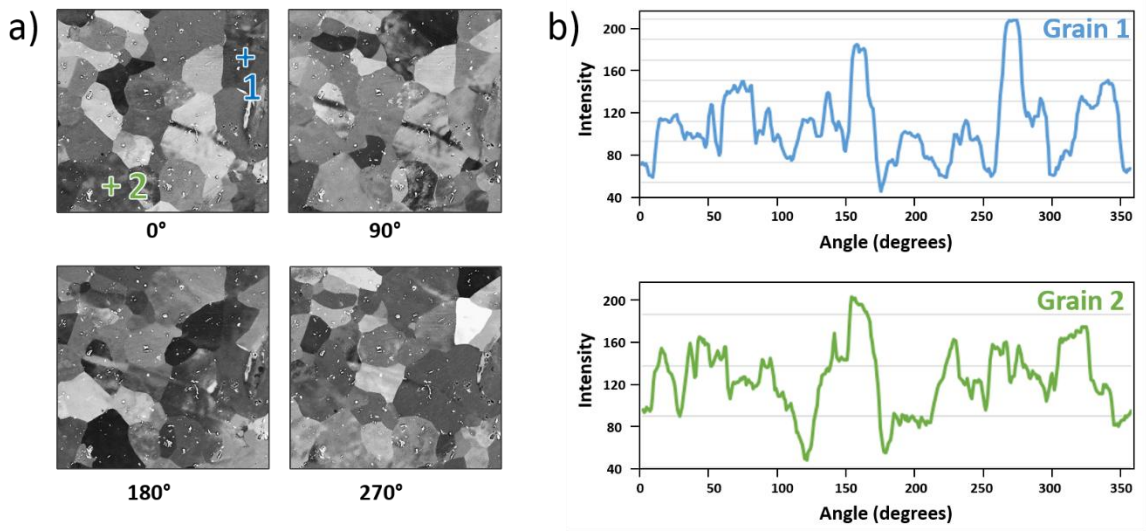

Figure 2: a) representative images extracted from the aligned stack; b) experimental intensity profiles extracted from the stack at two different positions.

From such experimental profiles, the orientation can be recovered through the following procedure: 1/ sampling of the orientation space, 2/ simulation of theoretical intensity profiles for each orientation of the sampling, 3/ search into this database to find the best match between experimental and theoretical profiles using dot product as metric. Sampling of the orientation space is carried out statistically by randomly generating 1 million quaternions on unit quaternions sphere using the algorithm described in reference [11] and taking into account the symmetry operations of the crystal. The mean disorientation between nearest neighbors in the orientation space is 0.5 degrees. Simulated profiles are calculated from theoretical Electron Channeling Pattern (ECP). Actually, during an ECP acquisition, the diffracted intensity is plotted as a function of the orientation of the beam relative to the sample normal. If the sample normal is parallel to the electron beam, its diffracted intensity will be found at the center of the ECP (called P in Fig. 3). In our configuration the sample is tilted at 10° with respect to the electron beam, thus the diffracted intensity is described by a 10° shift of point P to P' on the ECP. Therefore, the intensity profile, as a function of the rotation angle, corresponds to the intensity gathered along a 10° radius circle centered on point P. A tilt of 10 degrees together with a tension of 15kV is a good compromise to cross enough Kikuchi lines to obtain a unique signature of the orientation. ECP patterns were calculated using EMsoft simulation suite from M. De Graef *et al.* [12]. For each of the orientations, an ECP was computed, with parameters corresponding to the high tension, the tilt angle and the materials used. This leads to 1 million ECPs with a pattern size of 261x261 pixels and an opening semi-angle of 13° leading to a pixel resolution of 0.1°. The computation of the ECP database took 45 minutes on 8 cores Intel® Core™ i7-CPU @ 2.60GHz workstation. Because the electron beam is convergent, directions of incident electrons

belong to a cone of semi-angle alpha that depends on both aperture size and working distance. Electrons intensities as a function of the incident angle inside the cone are modelled by a Gaussian distribution of standard deviation sigma [13]. Therefore, instead of taking the intensity of a unique point on the circle drawn on the ECP, one has to integrate the intensity in the vicinity with the same Gaussian ponderation. An identical result is obtained by taking a unique point on an ECP Gaussian-blurred with the same sigma. In the present work, the sigma value of the Gaussian distribution depends on aperture diameters and working distance. Its value of 0.08° was determined using data available in Zaefferer *et al.* [14]. For each calculated ECP a unique theoretical profile, corresponding to one orientation, is extracted. This process is repeated for each of the 1 million ECP generated. Fig. 3b) shows a comparison of an experimental eCHORD intensity profile and a simulated one for a given orientation of the crystal.

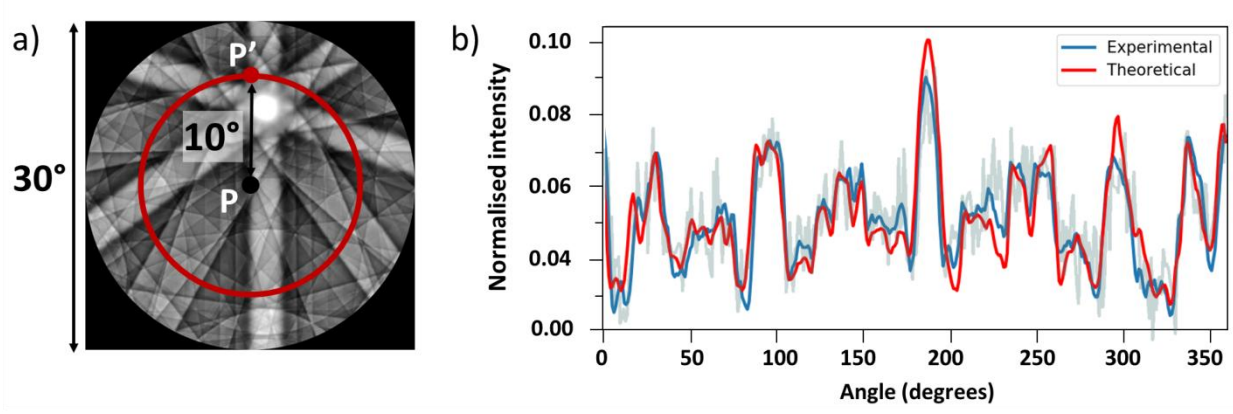

Figure 3: Modelling of the intensity profile for orientation (300.7°, 40.6°, 6.7°). a) ECP simulated from EMsoft at 15 kV for aluminum: in red, circle corresponding to the beam path when a sample is tilted at 10° and rotated from 0° to 360°; b) comparison between the theoretical

profile extracted from the ECP in (a) (red), the experimental profile before denoising (light blue) and after denoising (blue).

3. Results and Discussion

Fig. 4 presents a comparison between EBSD and eCHORD data on the same area of a polycrystalline aluminum alloy sample, with a database of 1 000 000 theoretical profiles. The EBSD map has been acquired with a Nordlys F camera and data were post-processed with HKL Channel5 software (Oxford Instruments, Abingdon, UK). EBSD mapping was performed with an accelerating voltage of 20kV, with a step of 400nm and a size of 498x509 pixels. The sampling of the pattern was 106x80 pixels whereas the resolution of the Hough transform was of 65. The acquisition speed was 283 Hz (leading to an acquisition of 15 minutes) for a hit rate of 92.8%. The eCHORD map has been obtained from an image series of 360 images corresponding to a 360° rotation of the stage. Each image has been acquired at 15kV, 10° tilt, with a beam scan speed of 10 seconds per image (leading to an acquisition of 1 hour) and a step size of 400nm. Rotation and acquisition of images processes were automated. Size of the region of interest after processing is 405x387 pixels. By nature, the hit rate is 100%. To have an idea about the confidence of the indexation, one can refer to the 'distance map' (Fig 4.d) which corresponds to one minus the dot product between the experimental profile and the assigned theoretical profile. Considering that acquisition and database generation were carried out simultaneously, the total time to obtain this eCHORD map was approximately 100 minutes: 1 hour for acquisition and database generation + 30 minutes for image processing and 5 minutes of indexation (~500 experimental profiles indexed per second). The disorientations angles between

EBSD reference map (after denoising) and eCHORD map follow a log-normal distribution peaked at 0.74 degree. Almost all grains are correctly indexed with an error of less than one degree compared to EBSD data. One has to keep in mind that such a point-to-point comparison is subject to angular and spatial imprecisions that occur when moving from EBSD acquisition geometry to the eCHORD one.

Concerning the angular resolution, the sampling of the orientation space, and therefore the size of the database, needs to be at least 1 million, otherwise some experimental profiles are not found in the database. This observation could witness an angular resolution potentially better than 0.5°, which is the mean disorientation between two neighbour orientations in the database. However, a limitation arises at low magnification due to the scanning of the region of interest which provokes a beam deflection. Depending on beam position during scanning, the angle between the rotation axis and the electron beam slightly differs from 10°. Many other parameters also influence the spatial resolution such as pixel size, accelerating voltage, sample tilt and quality of image alignment. Their respecting roles will be discussed in another paper.

Compared to all existing orientation mapping methods, eCHORD opens new perspectives. Firstly, the acquisition geometry is very simple (tilt of ~10° and 6mm for WD). This allows movements of the sample on a large scale without touching the electron column, which is definitely an advantage when mapping and stitching large areas. Another advantage linked to this geometry is the possibility to acquire 3D orientation volume (potentially on any given location on the surface of the sample) by coupling eCHORD with an ion column. Last but not least, the eCHORD method only requires standard BSE detector and goniometer, and can be implemented on any standard SEM.

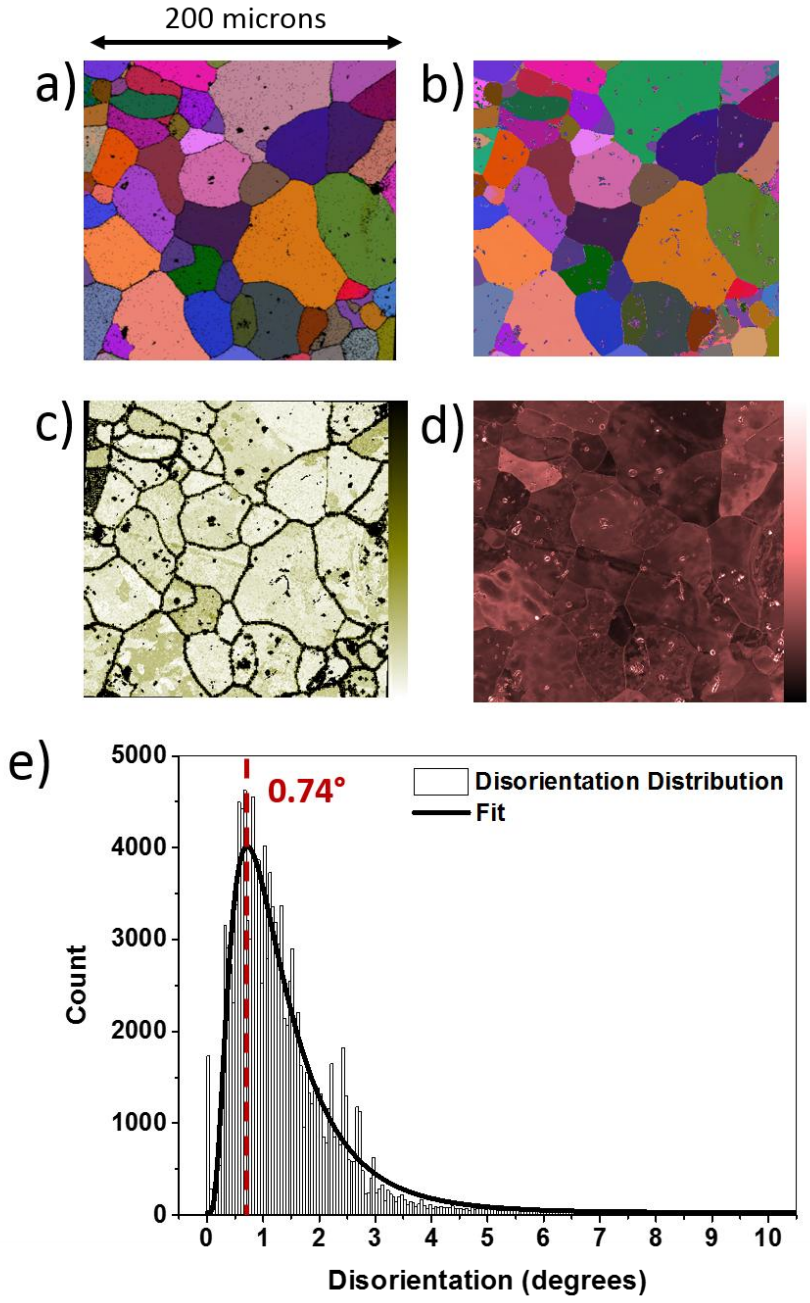

Figure 4: a) processed EBSD reference map (Euler map); b) eCHORD map (Euler angles) of the same area; c) Disorientation map from 0° (white) to 10° (black) between EBSD and eCHORD map; d) Distance map corresponding to 1 – dot product(experimental profiles; assigned

theoretical profile) from 0 (black – confident indexation) to 0.05 (white – less confident indexation); and e) corresponding disorientation distribution.

4. Conclusion

This proof-of-concept study shows that orientation maps can be obtained using BSE channeling contrast. Similar results within an error of 1° were obtained using eCHORD and EBSD techniques on aluminum alloy sample. Concerning acquisition and indexation time, it is worth noting that, in this proof-of-concept, it was not our goal to optimize them. Many improvements directions exist to reduce the time while keeping the performances: reducing numbers of images, increasing scan speed coupled with efficient denoising, selecting only pertinent beam directions in the ECP, improving database search algorithm... Further experiments will also be carried out to evaluate how eCHORD can be used for non-cubic, multi-phased or deformed materials. One main advantage of eCHORD is that no additional hardware is necessary for this method: standard BSE detector and goniometer are sufficient. Our set-up will potentially improve spatial resolution and acquisition time and may even open new perspectives towards 3D orientation imaging.

References

[1] A.J. Wilkinson, G. Meaden, D.J. Dingley, High resolution mapping of strains and rotations using electron backscatter diffraction, Materials Science and Technology. 22 (2006) 1271–1278. doi:10.1179/174328406x130966.

[2] E. Brodu, E. Bouzy, J.-J. Fundenberger, J. Guyon, A. Guitton, Y. Zhang, On-axis TKD for orientation mapping of nanocrystalline materials in SEM, Materials Characterization. 130 (2017) 92–96. doi:10.1016/j.matchar.2017.05.036.

[3] C. Langlois, T. Douillard, H. Yuan, N.P. Blanchard, A. Descamps-Mandine, B.V. de Moortèle, C. Rigotti, T. Epicier, Crystal orientation mapping via ion channeling: An alternative to EBSD, Ultramicroscopy. 157 (2015) 65–72. doi:10.1016/j.ultramic.2015.05.023.

[4] L. Reimer, Scanning Electron Microscopy, Springer Berlin Heidelberg, 1985. doi:10.1007/978-3-662-13562-4.

[5] J. Schindelin, I. Arganda-Carreras, E. Frise, V. Kaynig, M. Longair, T. Pietzsch, S. Preibisch, C. Rueden, S. Saalfeld, B. Schmid, J.-Y. Tinevez, D.J. White, V. Hartenstein, K. Eliceiri, P. Tomancak, A. Cardona, Fiji: an open-source platform for biological-image analysis, Nature Methods. 9 (2012) 676–682. doi:10.1038/nmeth.2019.

[6] B. Münch, Xlib plugins for FIJI software, accessible in 2017 at http://imagej.net/Xlib

[7] B. Busse, MultiStackReg plugin for FIJI software, accessible in 2017 at http://bradbusse.net/sciencedownloads.html

[8] D. Tschumperlé, R. Deriche, Anisotropic Diffusion Partial Differential Equations in Multi-Channel Image Processing : Framework and Applications., in: Advances in Imaging and Electron Physics (AIEP), Academic Press, 2007: pp. 145–209. https://hal.archives-ouvertes.fr/hal-00332798.

[9] J. Canny, A Computational Approach to Edge Detection, IEEE Transactions on Pattern Analysis and Machine Intelligence, PAMI-8 (1986) 679-698. doi: 10.1109/tpami.1986.4767851.

[10] P. Thevenaz, U.E. Ruttimann, M. Unser, A pyramid approach to subpixel registration based on intensity, IEEE Transactions on Image Processing. 7 (1998) 27-41. doi: 10.1109/83.650848.

[11] A. Morawiec, Orientations and Rotations – Chapter 5, Springer Berlin Heidelberg, 2004. doi:10.1007/978-3-662-09156-2.

[12] S. Singh, M.D. Graef, Dictionary Indexing of Electron Channeling Patterns, Microscopy and Microanalysis. 23 (2017) 1–10. doi:10.1017/s1431927616012769.

[13] J.I. Goldstein, D. E. Newbury, P. Echlin, D.C. Joy, C.E. Lyman, E. Lifshin, L. Sawyer, J.R. Michael, Scanning Electron Microscopy and X-ray Microanalysis, Springer US, 2003. doi: 10.1007/978-1-4615-0215-9.

[14] S. Zaefferer and N.-N. Elhami, Theory and application of electron channelling contrast imaging under controlled diffraction conditions, Acta Materialia. 75 (2014) 20-50. doi: 10.1016/j.actamat.2014.04.018.